# A New Family of 3d-4f Bis-Calix[4]arene-Supported Clusters

# A New Family of 3*d*-4*f* Bis-Calix[4]arene-Supported Clusters

Marco Coletta,[a] Ross McLellan,[a] Sergio Sanz,[b] Kevin J. Gagnon,[c] Simon J. Teat,[c] Euan K. Brechin*[b] and Scott J. Dalgarno*[a]

**Abstract:** Calix[4]arenes are versatile ligands that, whilst also serving other purposes, can act as platforms for the synthesis of a wide range of 3*d*, 4*f* and 3*d*–4*f* polymetallic clusters. The empirical metal ion binding rules established for calix[4]arene are closely mirrored by bis–calix[4]arene, a relatively new ligand in which two equivalents of the former are directly tethered at a methylene bridge position. The direct tethering within bis-calix[4]arene gives rise to some structural features that are related to calix[4]arene coordination chemistry, but the prevailing clusters have fascinating new topologies and coordination behaviors. Here we present the synthesis of a family of new bis-calix[4]arene-supported 3*d*–4*f* clusters, as well as their structural characterization and magnetic properties. Comparison is drawn with calix[4]arene coordination chemistry, showing logical extension of common structural fragments and cluster capping behaviors upon moving to bis-calix[4]arene. This approach therefore holds great potential for tuning cluster formation and composition at a high level through subsequent ligand alteration.

## Introduction

The synthesis of complex metallosupramolecular assemblies / polymetallic clusters can be achieved via several strategies that range from serendipitous formation through to directed assembly. The latter, that can alternatively be termed rational design, typically relies on the synthesis of ligands or building blocks that possess particular structural characteristics and / or chemical functionalities.[1] These properties subsequently allow the chemist to employ specific metal ion binding modes in order to impart topologically directing character, representing a generally preferred route towards the isolation of challenging multi-component assemblies. This approach can also be used to control and / or tune the chemical and physical properties[2] of the resulting assembly by exerting strong influence over cluster composition. The result of such control is the generation of new polymetallic clusters that are well understood and that have potential application in many areas of research; examples include their use as Single Molecule Magnets (SMMs),[3] catalysts[4] and host-guest systems.

Calix[4]arenes (general notation C[4] hereafter) have been used widely in supramolecular chemistry, the reasons for which include their possessing interesting conformational properties, the ease with which one can synthetically modify the upper- and / or lower-rims,[5] their propensity to act as hosts for suitably sized guests, and the fact that the polyphenolic lower-rim can bind 3*d* / 4*f* metal ions and form polymetallic clusters through phenolate bridging.[6] We (amongst others) have been actively exploring C[4] lower-rim coordination chemistry and related cluster formation, and in doing so have established an extensive library of 3*d*, 4*f* and 3*d*–4*f* clusters.[7] Our first result in this area was the synthesis of a series of $[Mn^{III}_2Mn^{II}_2(OH)_2(C[4])_2]$ SMMs displaying the common butterfly-like $\{Mn^{III}_2Mn^{II}_2(OH)_2\}$ core (Fig. 1A),[8] but with the oxidation state distribution reversed relative to the majority of analogous cluster core topologies found in the literature.[9] In this cluster type the body Mn cations are in a 2+ oxidation state, whereas those bound by the C[4] tetraphenolic pocket are in a 3+ oxidation state and occupy the wing-tip positions. The wing-tip $[Mn^{III}(C[4])]^-$ moiety caps the cluster core on each side, and this is in fact a recurring feature in C[4]-supported coordination chemistry; to date we have found that $[TM^{III}(C[4])]^-$, $[TM^{II}(C[4])]^{2-}$ or $[Ln^{III}(C[4])]^-$ moieties act as capping vertices, with C[4] oxygens bridging to metal ions within the cluster core.

We recently found that it is possible to replace one or both of the body $Mn^{II}$ ions in the aforementioned cluster with $Ln^{III}$ ions through variation in the metal salt, stoichiometries and reaction conditions employed; this afforded structurally related butterflies having $\{Mn^{III}_2Mn^{II}Ln^{III}(OH)_2\}$ and $\{Mn^{III}_2Ln^{III}_2(OH)_2\}$ cores respectively.[10] Analogous reactions carried out in the absence of $TM^{II/III}$ ions afforded C[4]-supported $Ln^{III}_6$ octahedra,[11] and a series of $Mn^{III}_4Ln^{III}_4$ clusters (Fig. 1B) were also obtained when using both TM and Ln ions.[12] The latter are best described as a square of $Ln^{III}$ ions capped on each edge by four $[Mn^{III}(C[4])]^-$ moieties, and these behave as SMMs or molecular refrigerants depending on the lanthanide employed. Finally, treatment of C[4] with copper(II) nitrate trihydrate afforded enneanuclear clusters (Fig. 1C) that have a tri-capped trigonal prismatic topology.[13] These clusters display interesting versatility in anion binding within the trigonal prismatic core, and $[Cu^{II}(C[4])]^{2-}$ moieties cap each face of the polyhedron. Analysis of this library of clusters has allowed us to establish metal ion binding rules for C[4] as follows: 1) $Mn^{III}$ is preferentially bound over other TM and Ln ions; 2) $TM^{II}$ ions (e.g. $Cu^{II}$) are preferentially bound over $Ln^{III}$ ions in the absence of $TM^{III}$ ions (e.g. $Mn^{III}$); 3) $Ln^{III}$ ions will be bound in the absence of both $TM^{II}$ and $TM^{III}$ ions.[14]

With these rules in mind, we recently began investigations into cluster formation with bis-*p*-$^t$Bu-calix[4]arene (bis-C[4]), a relatively new ligand comprising two C[4]s directly linked *via* the methylene bridge.[15] This is of particular interest considering that, akin to C[4], bis-C[4] would be conformationally flexible, but it could also act as a *double* capping species upon complexation

[a] Dr M. Coletta, Dr R. McLellan, Dr S. J. Dalgarno*
Institute of Chemical Sciences, Heriot-Watt University, Riccarton, Edinburgh, EH14 4AS, UK
E-mail: S.J.Dalgarno@hw.ac.uk
[b] Dr Sergio Sanz, Prof. E. K. Brechin*
EaStCHEM School of Chemistry, David Brewster Road, The University of Edinburgh, Edinburgh, EH9 3FJ, UK.
E-mail: E.Brechin@ed.ac.uk
[c] Dr K. J. Gagnon, Dr S. J. Teat
Advanced Light Source, Lawrence Berkeley National Laboratory Berkeley, CA 947240, USA.

Supporting information for this article is given via a link at the end of the document.

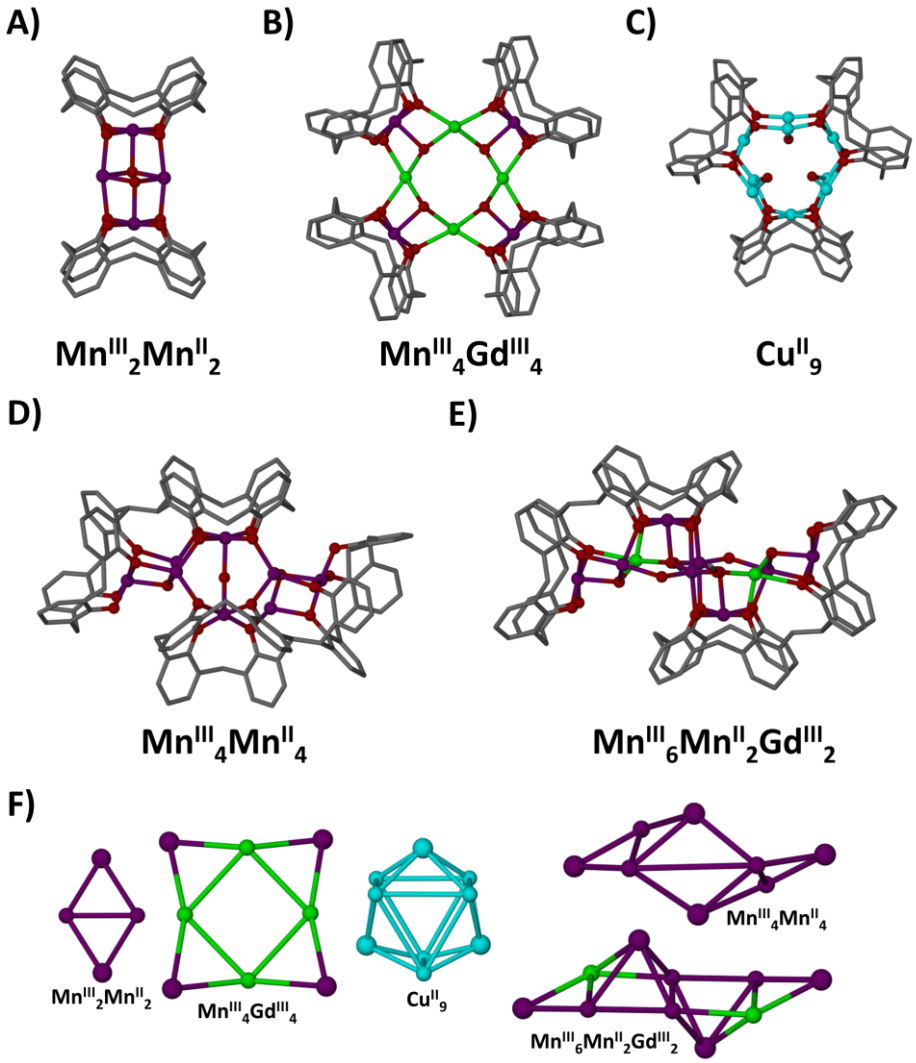


**Figure 1.** Structures of selected polymetallic C[4]- and bis-C[4]-supported clusters. A) Cluster supported by two C[4]s and with metal ions arranged in butterfly-like topology.[8] B) Square within square $Mn^{III}_4Gd^{III}_4$ cluster supported by four C[4]s.[12] C) Tri-capped trigonal prismatic $Cu^{II}_9$ cluster, with the molecule shown along the $C_3$ axis of the prismatic core.[13] D) Bis-C[4]-supported $Mn^{III}_4Mn^{II}_4$ cluster showing two fused and distorted butterflies.[17] E) Bis-C[4]-supported $Mn^{III}_6Mn^{II}_2Ln^{III}_2$ cluster obtained *via* stoichiometric control.[18] F) Metallic skeletons of the clusters shown in A – E with single or double capping moieties represented by large spheres. Colour code: Mn – purple, Cu – light blue, Ln – green, C – grey, O – red. C[4] / Bis-C[4] $^t$Bu groups, H atoms, some bridging anions and ligated solvent have been omitted for clarity in A – E.

with suitable metal ions.[16] Initial investigations conducted with bis-C[4] showed that the established binding rules were indeed maintained upon metal ion complexation, and the first cluster isolated was a $[Mn^{III}_4Mn^{II}_4(bis\text{-}C[4])_2]$ species that can be visualized as two distorted and fused $\{Mn^{III}_2Mn^{II}_2\}$ cores (compare Fig. 1A and 1D).[17] Structural differences between these two related clusters are primarily due to methylene bridge linking, and in this case two $Mn^{II}$ ions occupy binding sites between the two C[4] moieties. In this regard, it should be noted that the free ligand exists as an up-down antiparallel arrangement of C[4] (Fig. S1), and inversion gives rise to these new metal ion binding sites between their polyphenolic lower-rims. As is the case for $[Mn^{III}_2Mn^{II}_2(OH)_2(C[4])_2]$, the $Mn^{II/III}$ ions in the bis-C[4]-supported cluster are linked through bridging phenolates and hydroxides. The second cluster to emerge from this exploratory chemistry was a $[Mn^{III}_4Mn^{II}_2Gd^{III}_2(bis\text{-}C[4])_2]$ species that is a structural relative of the aforementioned $Mn_8$ cluster (compare Fig. 1D and 1E),[17] the main difference being the interchange of two $Mn^{II}$ for $Ln^{III}$ ions; this behavior is a close parallel to that described above for C[4],[10] further suggesting that methylene bridge linking is a viable route to the logical extension of metal ion binding rules / behaviors for multi-component systems. We recently showed that, as in C[4]-supported cluster chemistry, variation in reaction stoichiometry has a dramatic effect on the assembly of bis-C[4]-supported clusters. Exploration of this variable led to the isolation of two new clusters, $[Mn^{III}_6Mn^{II}_4(bis\text{-}C[4])_2]$ and $[Mn^{III}_6Mn^{II}_2Gd^{III}_2(bis\text{-}C[4])_2]$, the cores of which have been 'expanded' through the incorporation of two additional central $Mn^{III}$ ions in each case relative to their $[Mn^{III}_4Mn^{II}_4(bis\text{-}C[4])_2]$ and $[Mn^{III}_4Mn^{II}_2Gd^{III}_2(bis\text{-}C[4])_2]$ relatives respectively.[18]

Given the structural trends observed upon moving from C[4] to bis-C[4], it is clear that the metal ion binding rules established for the former translate to the latter. Here we report the isolation, characterization and magnetic properties for three new $TM^{II/III}_xLn^{III}_y$bis-C[4]-supported clusters incorporating either $Cu^{II}$, $Fe^{III}$ or $Mn^{III}$ ions, representing a significant addition to the library of known cluster types with this ligand. The established binding rules again translate for these metal ions, further suggesting that the linkage of calix[*n*]arenes of varying ring size represents a burgeoning area of research for investigation.

## Results and Discussion

Reaction of bis-C[4] with copper(II) and terbium(III) nitrate hydrates in a DMF / MeOH mixture (to aid bis-C[4] solubility) and in the presence of $Et_3N$ as a base afforded single crystals of formula $[Cu^{II}_4Tb^{III}_5(bis\text{-}C[4])_2(\mu_3\text{-}OMe)(\mu\text{-}OMe)(\mu_3\text{-}OH)(\mu_4\text{-}NO_3)(\mu_5\text{-}NO_3)(MeOH)(dmf)_6(H_2O)_4](OH)_2(dmf)_6(H_2O)$, **1**, upon slow evaporation of the mother liquor. The crystals were found to be in a monoclinic cell and structure solution was carried out in

the space group $P2_1/n$. The asymmetric unit comprises two bis-C[4]s housing a $Cu^{II}_4Tb^{III}_5$ metallic core, the cations in which are bridged by hydroxide and nitrate anions (Fig. 2). The four $Cu^{II}$ ions are located in the fully deprotonated lower-rim bis-C[4] phenolato pockets (Cu–O bond lengths in the range of 1.906(7) – 2.031(7) Å) and their coordination spheres are completed by $\mu_3$-hydroxide, $\mu_3$-methoxide and $\mu_5$-nitrate anions (Cu-O bond lengths in the range of 2.202(7) – 2.239(7) Å). These anions bridge to the five $Tb^{III}$ ions (Tb–O bond lengths in the range of 2.260(7) – 2.494(7) Å), four of which are seven coordinate (distorted pentagonal bipyramidal geometries) and are located in the binding sites generated by inversion of the bis-C[4] ligands. The remaining $Tb^{III}$ ion (Tb3) is octacoordinate, has distorted square antiprismatic geometry and links the two $[Cu^{II}_2Tb^{III}_2$(bis-C[4])] fragments, and is located near-equidistant from these two moieties; the distances found between Tb3 and the centroids generated by each $[Cu^{II}_2Tb^{III}_2$(bis-C[4])] fragment are both ~ 4.7 Å. All of the $Tb^{III}$ ions are bound to the aforementioned bridging anions, bis-C[4] oxygens (Tb–O bond lengths in the range of 2.279(6) – 2.385(7) Å) and ligated solvent molecules (dmf, MeOH or $H_2O$, with Tb–O bond lengths in the range of 2.304(7) – 2.397(8) Å). Double capping behavior is observed as anticipated, in this case with two $[Cu^{II}_2$(bis-C[4])$]^{4-}$ moieties encapsulating two $Tb^{III}$ cations residing within the binding pockets originating from ligand inversion (Fig. 2B). Symmetry expansion of the structure of **1** does not show any significant interaction between the metal clusters, and co-crystallized dmf molecules occupy space between symmetry equivalents (s.e.) along the *a* and *c* axes. The closest metal-metal intercluster distance is along the *b* axis and is ~12.9 Å between Cu1 and Cu4 of a s.e. cluster (Figure S2).

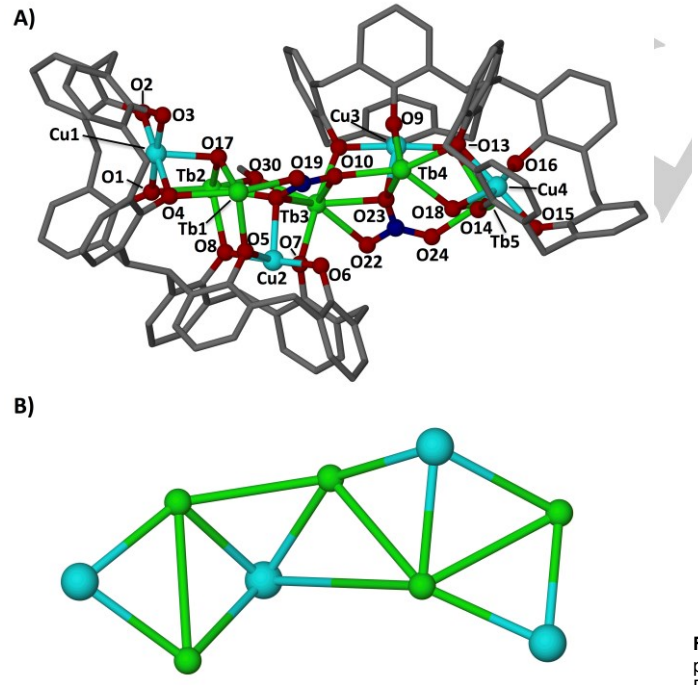


**Figure 2.** Views of the single–crystal X-ray structure of **1** showing the polymetallic $Cu^{II}_4Tb^{III}_5$ core. A) Two butterfly fragments are linked through a central $Tb^{III}$ ion and bridging nitrates. B) Metallic skeleton of **1** with the capping $[Cu^{II}$(TBC[4])$]^{2-}$ moieties drawn as large spheres. The view in B is a 90º rotation of A. Bis-C[4] $^t$Bu groups, H atoms and ligated solvent molecules omitted for clarity. Colour code: Cu – light blue, Tb – green, C – grey, N – blue, O – red.

Treatment of bis-C[4] with iron(III) and gadolinium(III) nitrate hydrates in a DMF / MeOH mixture in the presence of $Et_3N$ as a base afforded single crystals of formula $[Fe^{III}_5Gd^{III}_4$(bis-C[4])$_2(\mu_4$-O$)_2(\mu_3$-O$)_2(\mu_3$-$NO_3)_2$(dmf)$_8(H_2O)_6$](OH), **2**, upon slow evaporation of the mother liquor. The crystals were found to be in a triclinic space group and structure solution was carried out in the space group *P*-1. The asymmetric unit comprises a distorted $Fe^{III}_2Gd^{III}_2$ butterfly housed within a bis-C[4], and a $Fe^{III}$ ion linked to the aforementioned butterfly *via* bridging nitrate and oxo anions. Symmetry expansion around the inversion center gives rise to the whole cluster shown in Figure 3A. As can be seen by inspection, two $[Fe^{III}_2Gd^{III}_2$(bis-C[4])] butterflies / fragments are linked by the near-central $Fe^{III}$ cation that sits just away from the aforementioned center of inversion, located between the two cluster fragments. This $Fe^{III}$ ion and the bridging nitrates are disordered over two positions (one position shown in Fig. 3A) and this disorder was successfully modelled using partial occupancies; only one position is discussed here for the sake of brevity.

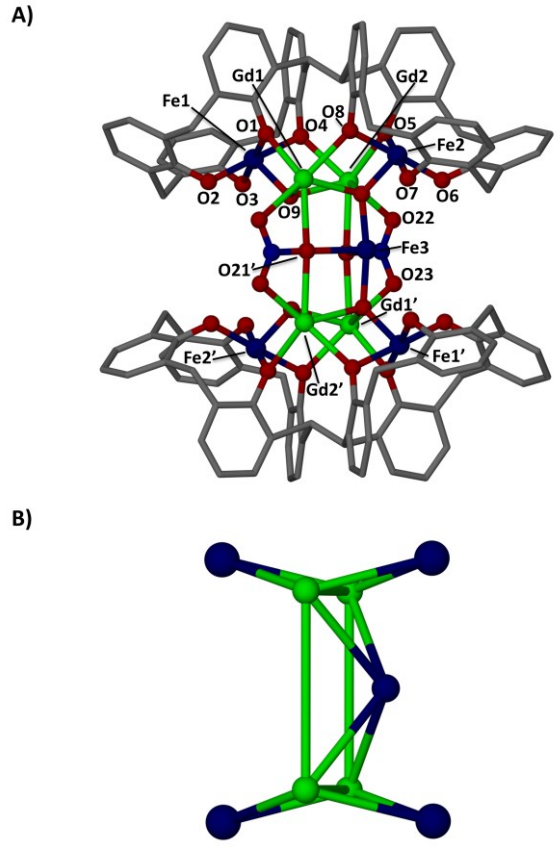


**Figure 3.** Views of the single–crystal X-ray structure of **2** showing the polymetallic $Fe^{III}_5Gd^{III}_4$ core. A) Two butterfly fragments linked through a central $Fe^{III}$ ion and bridging nitrates/oxides. B) Metallic skeleton of **2** showing edge capping by $[Fe^{III}$(TBC[4])$]^-$ moieties (drawn as large spheres), $Gd^{III}$ ions arranged in a square and face capping by the central $Fe^{III}$ ion. Bis-C[4] $^t$Bu groups, H atoms and ligated solvent molecules omitted for clarity. Colour code: Fe – dark blue, Gd – green, C – grey, N – blue, O – red.

Fe1, Fe2, and their symmetry equivalents are all hexacoordinate, have distorted octahedral geometries, and reside in the fully deprotonated lower-rim bis-C[4] phenolato pockets (Fe–O bond lengths in the range of 1.955(4) – 2.029(4) Å); this is expected based on the metal ion binding rules outlined in the introductory section. The Fe1 / Fe2 coordination spheres are completed by ligated dmf molecules that reside in the bis-C[4] cavities (Fe1–O11, 2.091(8) Å and Fe2–O12, 2.108(6) Å) and $\mu_4$-O anions (Fe1–O9, 1.942(6) Å and Fe2–O10, 1.938(5) Å) that bridge to Gd1 and Gd2 (Gd–O bond lengths in the range of 2.372(5) – 2.403(6) Å). Both Gd1 and Gd2 are octacoordinate, have distorted square antiprismatic geometries, and are located in the binding pockets generated by bis-C[4] inversion. Each $Gd^{III}$ ion is bound to two bis-C[4] oxygen atoms (Gd–O bond lengths in the range of 2.351(4) – 2.385(5) Å), two oxygen atoms of a $\mu_3$-$NO_3$ anion (Gd–O bond lengths in the range of 2.276(8) – 2.564(4) Å) and ligated solvent molecules (Gd–O bond lengths in the range of 2.356(7) – 2.572(12) Å). Finally, Fe3, located near the center of the cluster, bridges the two $[Fe^{III}_2Gd^{III}_2$(bis-C[4])] butterflies / fragments as outlined above, and caps one face of the square described by the $Gd^{III}$ cations. The Fe3 coordination sphere is completed by two $\mu_4$-O anions (Fe3–O10, 1.972(4) Å and Fe3–O9', 2.039(5) Å), oxygens from two $\mu_3$-$NO_3$ anions (Fe3–O21, 2.247(5) Å and Fe–O21', 2.265(5) Å) and two aqua ligands (Fe3–O16, 2.016(10) Å and Fe3–O17, 2.019(10) Å). The $Gd^{III}$ square is also capped on each edge by a $[Fe^{III}_2$(bis-C[4])$]^{2-}$ moiety in line with the expected double capping behavior of bis-C[4]; the capped $Gd^{III}$ square is also a recurring structural motif when considering previously reported C[4]-supported metal clusters, although in this case double capping occurs in an alternative manner around the central core.[12] Symmetry expansion of the structure of **2** reveals weak Van der Waals interactions along the *c* axis between the dmf molecule ligated to Gd2 and its s.e.; this occurs with a distance between nitrogen atoms of ~3.7 Å. The closest metal-metal intercluster distances were also found along the *c* axis, occurring between Gd2 and its s.e. with a distance of ~11.2 Å. The next shortest metal-metal intercluster distance of note is between Fe3 and Gd2 from a s.e. cluster, occurring with a distance of ~13.9 Å (Figure S3).

Reaction of bis-C[4] with manganese(II) and gadolinium(III) chlorides in a DMF / MeOH mixture and in the presence of $Et_3N$ as a base afforded single crystals of formula $[Mn^{III}_4Gd^{III}_4$(bis-C[4])$_2(\mu_3$-OH$)_4(\mu$-$CO_3)_2$(dmf)$_8(H_2O)_4$](MeOH)(dmf)$_2$, **3**, upon slow evaporation of the mother liquor. The crystals were found to be in a monoclinic cell and structure solution was carried out in the space group $P2_1/n$. The asymmetric unit comprises two distorted $[Mn^{III}_2Gd^{III}_2$(bis-C[4])] butterflies / fragments, and these are connected *via* carbonate bridges, likely resulting from fixation of atmospheric $CO_2$; this is a common phenomenon in Ln coordination chemistry[19] and has also been previously reported in C[4]-supported cluster chemistry. The four $Mn^{III}$ ions are in a distorted octahedral geometry and are located in the fully deprotonated lower-rim bis-C[4] phenolato pockets (Mn–O bond lengths in the range of 1.889(5) – 1.994(5) Å). Oxidation states were confirmed by bond valence sums (BVS), giving respective values of 3.16, 3.12, 3.32 and 3.08 for Mn1 – Mn4. Their coordination spheres are completed by ligated dmf molecules that reside in the C[4] cavities (Mn – O(dmf) bond lengths in the range of 2.152(6) – 2.239(5) Å) and $\mu_3$-OH anions that bridge each $Mn^{III}$ to the closest $Gd^{III}$ ion (Mn – O($\mu_3$-OH) bond lengths in the range of 2.002(5) – 2.130(4) Å); these ligands define the Jahn-Teller axis for each $Mn^{III}$ ion, details of which can be found in the supporting information (Figure S4). The four $Gd^{III}$ cations are octacoordinate, have square antiprismatic geometry, and reside in the binding regions generated by bis-C[4] inversion. Each $Gd^{III}$ cation is bound to two bis-C[4] oxygens (Gd–O bond lengths in the range of 2.331(5) – 2.523(5) Å), as well as ligated solvent molecules (Gd–O bond lengths in the range of 2.351(6) – 2.430(5) Å). These cations are bridged *via* the aforementioned $\mu_3$-OH anions (Gd–O bond lengths in the range of 2.322(5) – 2.434(5) Å) and oxygen atoms of carbonate bridges that are linking the two halves of the cluster (Gd–O range 2.393(5) – 2.480(5) Å). The metallic core in **3** is different to that found in **2**, perhaps due to the lack of a central bridging metal ion, and is best described as a distorted rectangle of $Ln^{III}$ ions, capped on the shorter sides by a $[Mn^{III}_2$(bis-C[4])$]^{2-}$ moiety. Again, the observation of persistent structural trends suggests that one may link >2 C[4]s via the methylene bridges to logically influence cluster formation and, potentially, the physical properties of the resulting assemblies.

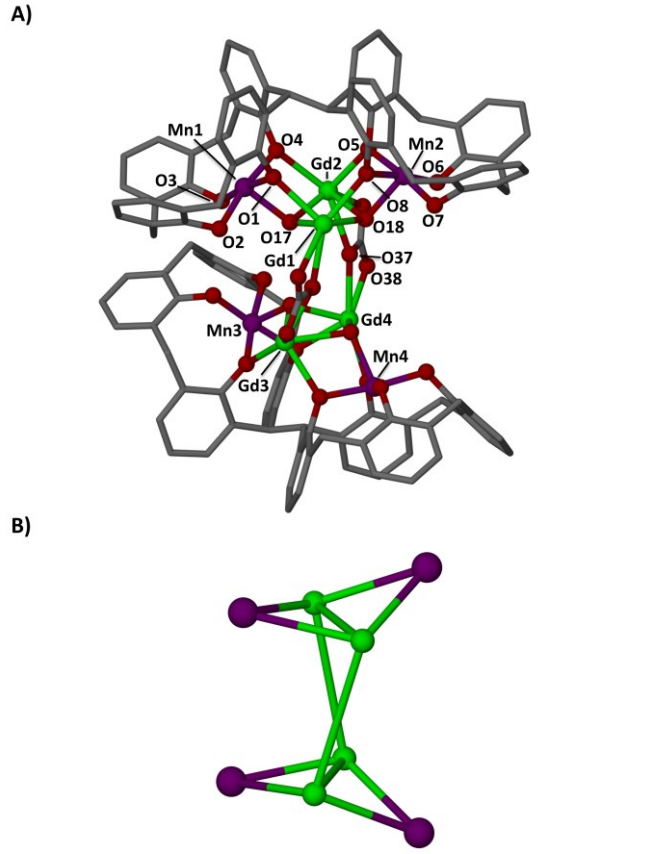


**Figure 4.** Views of the single–crystal X-ray structure of **3** showing the polymetallic $Mn^{III}_4Gd^{III}_4$ core. A) Two butterfly fragments linked through bridging carbonates. B) Metallic skeleton of **3** with the capping $[Mn^{III}$(TBC[4])$]^-$ moieties drawn as large spheres, and showing the $Gd^{III}$ ions arranged in a square. Bis-C[4] $^t$Bu groups, H atoms and ligated solvent molecules omitted for clarity. Colour code: Mn – purple, Gd – green, C – grey, O – red.

Symmetry expansion of the structure of **3** reveals that there are no significant intermolecular interactions occurring between the clusters. The shortest metal-metal intercluster distance is along the *a* axis, occurring between Gd1 and Gd4 of a s.e. cluster with a distance of ~12.8 Å (Figure S5). The second, comparable intercluster distance, occurs along the *b* axis between Mn2 and a s.e. Mn3 with a distance of ~13.0 Å.

**Magnetic properties**

The dc (direct current) molar magnetic susceptibility, $\chi_M$, of polycrystalline samples of **1-3** were measured in an applied magnetic field, *B*, of 0.1 T, over the *T* = 5-300 K temperature range. The experimental results are shown in Figure 5 in the form of the $\chi_M T$ product versus *T*, where $\chi_M = M / B$, and *M* is the magnetisation of the sample.

At room temperature, the experimentally observed $\chi_M T$ products of 60.8, 53.9 and 44.0 $cm^3$ K $mol^{-1}$ are consistent with the Curie constants for $[Cu^{II}_4Tb^{III}_5]$, $[Fe^{III}_5Gd^{III}_4]$ and $[Mn^{III}_4Gd^{III}_4]$ units, respectively. Upon cooling, the $\chi_M T$ product of compound **1** remains relatively constant until *T* ~ 175 K where the it begins to decrease slowly, reaching a value of 46.9 $cm^3$ K $mol^{-1}$ at *T* = 5 K. The data for complexes **2** and **3** are rather different, both $\chi_M T$ products remaining constant until approximately *T* = 50 K wherefrom they increase to maximum values of 57 (**2**) and 53 $cm^3$ K $mol^{-1}$. The behaviour in all three cases is consistent with competing (weak) ferro- and antiferromagnetic exchange interactions, with the decrease in $\chi_M T$ in **1** associated with the depopulation of ligand-field sublevels of the $Tb^{III}$ ions. The large nuclearities, complex topologies and the presence of the anisotropic $Tb^{III}$ ion prevents quantitative analysis of the exchange constants in these compounds, but some general comments can be made. Inspection of the structures of **1** (Figure 2) and **3** (Figure 4) shows there are no direct, ligand-mediated TM···TM (TM = transition metal) magnetic exchange pathways, only TM···Ln and Ln···Ln (Ln = lanthanide metal) contacts, both of which would be expected to be very weak. Indeed, previous measurements of calix[n]arene-based $TM^{II/III}$-$Gd^{III}$ clusters reveal exchange constants that are just a fraction of a wavenumber, with the shape of the $\chi_M T$ versus *T* curve for **3** being very similar to that observed for the C[4]-supported $[Mn^{III}_2Gd^{III}_2]$ species, where $J_{Mn\text{-}Gd}$ = +0.075 $cm^{-1}$ and $J_{Gd\text{-}Gd}$ = -0.006 $cm^{-1}$.[10]

Analysis of the magnetic data of compound **2** is further complicated by the presence of the central Fe3 ion which is disordered over two positions. While reported $Fe^{III}$-$Gd^{III}$ exchange constants in C[4]-supported cages are of the same magnitude as described above,[14d] $Fe^{III}$-O-$Fe^{III}$ exchange can be large, though strongly dependent on the $Fe^{III}$-Ô-$Fe^{III}$ angle, with the strongest AF exchange observed for a linear moiety and becoming less AF as the angle decreases.[20] The $Fe^{III}$-Ô-$Fe^{III}$ angles in **2** (Fe1-O9-Fe3; Fe3-O10-Fe2) are approximately 130º (with $\mu_4$-O9, $\mu_4$-O10 also bridging to two Gd ions), and inspection of Figure 5 suggests little evidence for the presence of strong TM···TM exchange. These observations are also consistent with low temperature variable-temperature-and-variable-field (VTVB) magnetisation data collected in fields of up to *B* = 7 T (Figure 5). While the magnetisation (Figure 6) of complex **1** does not saturate at *B* = 7 T (*M* = 26.4 $\mu_B$), those for complexes **2** (*M* = 48.0 $\mu_B$) and **3** (*M* = 41.6 $\mu_B$) are approaching that expected for the field-induced stabilisation of the maximum *S* = 53/2 and *S* = 22 states, respectively. There are no frequency-dependent signals in out-of-phase ($\chi_M''$) ac susceptibility for **1**-**3**, ruling out any SMM behaviour.

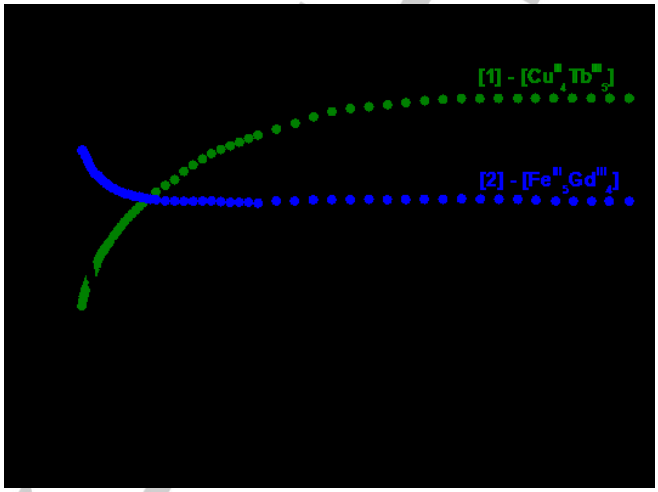


**Figure 5.** Plot of $\chi_M T$ versus *T*, for complexes **1**-**3** in a field of *B* = 0.1 T.

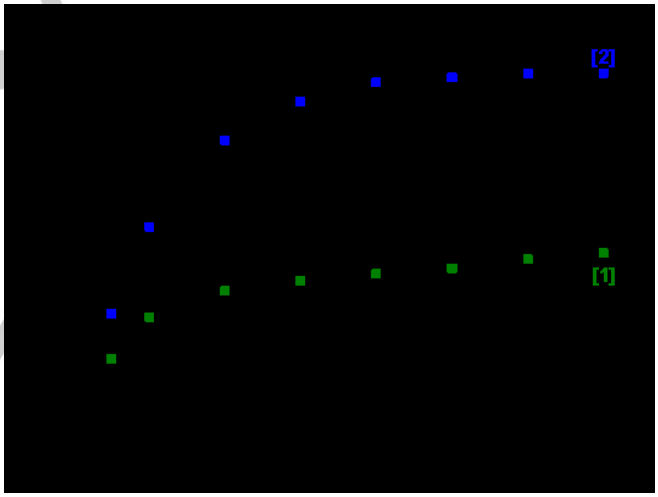


**Figure 6.** Plot of magnetisation (*M*) versus field (*B*) for complexes **1**-**3** at *T* = 2 K.

## Conclusions

In conclusion, our library of bis-C[4]-supported metal cluster has been significantly expanded in this contribution through the synthesis and characterization of three novel assemblies. Dc susceptibility and magnetization measurements reveal the presence of competing (and weak) ferro- and antiferromagnetic interactions in all three cases, consistent with the behavior of similar cages constructed with C[4]. Despite the complexity of the systems reported, the coordination modes observed / cluster topologies obtained are fully compliant with anticipated structure capping behavior, suggesting that further and logical extension of

ligand design principles should lead to the isolation of tailored, highly symmetric, high nuclearity clusters that will be of interest to many. Work continues with this goal in mind, but also with a view to understanding the influence of co-ligands on cluster formation with bis-C[4]. Results from these studies will be reported in due course.

## Experimental Section

Bis-C[4] was synthesised according to literature procedure.[15] Single crystal diffraction data were collected on a Bruker APEX II CCD diffractometer equipped with a PHOTON 100 detector operating at 100(15) K and using synchrotron radiation ($\lambda$ = 0.7749 Å). Supporting Information includes a figure showing the structure of bis-C[4], as well as videos showing rotating structures for **1** – **3**.

**Synthesis of $[Cu^{II}_4Tb^{III}_5(BisTBC[4])_2(\mu_3\text{-}OMe)(\mu\text{-}OMe)(\mu_3\text{-}OH)(\mu_4\text{-}NO_3)(\mu_5\text{-}NO_3)(MeOH)(dmf)_6(H_2O)_4](OH)_2(dmf)_6(H_2O)$, 1:** BisTBC[4] (350 mg, 0.27 mmol, 1eq.), $Cu(NO_3)_2{\cdot}3H_2O$ (65 mg, 0.27 mmol, 1 eq.) and $Tb(NO_3)_3{\cdot}6H_2O$ (245 mg, 0.54 mmol, 2 eq.) were suspended in a 1:1 DMF/MeOH mixture (20 mL) and stirred for 10 minutes. $Et_3N$ (0.35 mL) was added and the resulting brown solution was stirred for additional 2 h and filtered. The mother liquor was allowed to slowly evaporate, affording crystals suitable for *X*-ray diffraction studies. Elemental Analysis (%) calculated for **1**, $C_{215}H_{308}Cu_4Tb_5N_{14}O_{45}$ (M = 4857.73): C, 53.16%; H, 6.39%; N, 4.04%. Found: C, 52.84%; H, 6.21%; N, 3.78%. **Yield** 292 mg (22%). **Crystal data for 1 (CCDC 1560942):** $C_{215}H_{308}Cu_4N_{14}O_{45}Tb_5$, M = 4857.73, Orange needle, 0.3 x 0.02 x 0.01 mm$^3$, monoclinic, space group $P2_1/n$ (No. 14), $a$ = 19.0415(7), $b$ = 55.063(2), $c$ = 25.3349(9) Å, β = 97.974(2)º, $V$ = 26306.3(17) Å$^3$, $Z$ = 4, $2\theta_{max}$ = 48.34º, 32357 reflections collected, 32357 unique ($R_{int}$ = merged, $R_{sigma}$ = 0.0395). Final *GooF* = 1.026, $R_1$ = 0.0706, $wR_2$ = 0.1633 (all data).

**Synthesis of $[Fe^{III}_5Gd^{III}_4(BisTBC[4])_2(\mu_4\text{-}O)_2(\mu_3\text{-}O)_2(\mu_3\text{-}NO_3)_2(dmf)_8(H_2O)_6](OH)$, 2:** BisTBC[4] (350 mg, 0.27 mmol, 1 eq.), $Fe(NO_3)_3{\cdot}9H_2O$ (109 mg, 0.27 mmol, 1 eq.) and $Gd(NO_3)_3{\cdot}6H_2O$ (488 mg, 1.08 mmol, 4 eq.) were suspended in a 1:1 DMF/MeOH mixture (20 mL) and stirred for 10 minutes. $Et_3N$ (0.35 mL) was added and the resulting orange/brown solution was stirred for additional 2 h and filtered. The mother liquor was allowed to slowly evaporate, affording crystals suitable for *X*-ray diffraction studies. Elemental Analysis (%) calculated for **2**, $C_{200}H_{274}Fe_5Gd_4N_{10}O_{41}$ (M = 4382.69): C, 54.81%; H, 6.3%; N, 3.2%. Found: C, 54.56%; H, 6.09%; N, 3.18%. **Yield** 240 mg (20%). **Crystal data for 2 (CCDC 1560943):** $C_{200}H_{274}Fe_5Gd_4N_{10}O_{41}$, M = 4382.69, Orange block, 0.05 x 0.05 x 0.01 mm$^3$, triclinic, space group $P$-1 (No. 2), $a$ = 16.926(2), $b$ = 19.634(2), $c$ = 20.203(2)Å, $\alpha$ = 114.498(2)°, $\beta$ = 98.345(2)°, $\gamma$ = 99.663(2)°, $V$ = 5847.7(11) Å$^3$, $Z$ = 1, $2\theta_{max}$ = 58º, 65628 reflections collected, 23877 unique ($R_{int}$ = 0.0597, $R_{sigma}$ = 0.0691). Final *GooF* = 1.043, $R_1$ = 0.0594, $wR_2$ = 0.1863 (all data).

**Synthesis of $[Mn^{III}_4Gd^{III}_4(BisTBC[4])_2(\mu_3\text{-}OH)_4(\mu\text{-}CO_3)_2(dmf)_8(H_2O)_4](MeOH)(dmf)_2$, 3:** BisTBC[4] (350 mg, 0.27 mmol, 1 eq.), $MnCl_2{\cdot}4H_2O$ (107 mg, 0.54 mmol, 2 eq.) and $GdCl_3{\cdot}6H_2O$ (71 mg, 0.27 mmol, 1 eq.) were suspended in a 1:1 DMF/MeOH mixture (20 mL) and stirred for 10 minutes. $Et_3N$ (0.35 mL) was added and the resulting purple solution was stirred for additional 2 h and filtered. The mother liquor was allowed to slowly evaporate, affording crystals suitable for *X*-ray diffraction studies. Elemental Analysis (%) calculated for **3**, $C_{209}H_{290}Mn_4Gd_4N_{10}O_{41}$ (M = 4447.44): C, 56.44%; H, 6.57%; N, 3.15%. Found: C, 56.15%; H, 6.26%; N, 2.98%. **Yield** 396 mg (33%).

**Crystal data for 3 (CCDC 1560944):** $C_{212.6}H_{302}Gd_4Mn_4N_{11}O_{43.5}$, M = 4556.59, Purple needle, 0.3 x 0.07 x 0.01 mm$^3$, monoclinic, space group $P2_1/n$ (No. 14), $a$ = 17.7206(8), $b$ = 41.6212(17), $c$ = 33.0584(14) Å, β = 102.014(2)º, $V$ = 23848.3(18) Å$^3$, $Z$ = 4, $2\theta_{max}$ = 54.448º, 40784 reflections collected, 40784 unique ($R_{int}$ = merged, $R_{sigma}$ = 0.0524). Final *GooF* = 1.085, $R_1$ = 0.0690, $wR_2$ = 0.1765.

## Acknowledgements

We thank the EPSRC (RM / EKB /SJD, I031421 / I03255X) and Heriot-Watt University (MC, James Watt Studentship) for financial support of this work. The Advanced Light Source is supported by the Director, Office of Science, Office of Basic Energy Sciences, of the US Department of Energy under contract no. DE-AC02-05CH11231.

**Keywords:** Calixarenes • Clusters • Coordination Chemistry • Magnetism • Coordination Modes

[1] For some examples see: a) J.-F. Ayme, J. E. Beves, D. A. Leigh, R. T. McBurney, K. Rissanen, D. Schultz, *Nat. Chem.* **2012**, *4*, 15; b) Q.-F. Sun, S. Sato, M. Fujita, *Angew. Chem. Int. Ed.* **2014**, *53*, 13510; *Angew. Chem.* **2014**, *126*, 13728; c) D. A. Leigh, R. G. Pritchard, A. J. Stephens, *Nat. Chem.* **2014**, *6*, 978; C. S. Wood, T. K. Ronson, A. M. Belenguer, J. J. Holstein, J. R. Nitschke, *Nat. Chem.* **2015**, *7*, 354.

[2] X. Yan, T. R. Cook, P. Wang, F. Huang, P. J. Stang, *Nat. Chem.* **2015**, *7*, 342.

[3] For some examples see: (*a*) G. Aromí and E. K. Brechin, *Struct. Bonding* **2006**, *122*, 1; (*b*) J.-N. Rebilly and T. Mallah, *Struct. Bonding* **2006**, *122*, 103.

[4] C. J. Brown, F. D. Toste, R. G. Bergman, K. N. Raymond, *Chem. Rev.* **2015**, *115*, 3012.

[5] C. D. Gutsche in *Calixarenes*, Kluwer Academic Publishers, Dordrecht, **2001**, Chapter 1 and references therein.

[6] Petrella, A. J.; Raston, C. L. J. *Organomet. Chem.* **2004**, *689*, 4125.

[7] M. Coletta, E. K. Brechin, S. J. Dalgarno in *Calixarenes and Beyond* , *Ch. 25*, (Eds.: P. Neri, J. L. Sessler and M. –X. Wang) , Springer International Publishing, Switzerland, 1st edn, **2016**, pp 671-689.

[8] a) G. Karotsis, S. J. Teat, W. Wernsdorfer, S. Piligkos, S. J. Dalgarno, E. K. Brechin *Angew. Chem. Int. Ed.*, **2009**, *48*, 8285; b) S. M. Taylor, G. Karotsis, R. D. McIntosh, S. Kennedy, S. J. Teat, C. M. Beavers, W. Wernsdorfer, S. Piligkos, S. J. Dalgarno, E. K. Brechin *Chem. Eur. J.*, **2011**, *17*, 7521.

[9] E. K. Brechin, J. Yoo, M. Nakano, J. C. Huffman, D. N. Hendrickson, G. Christou *Chem. Commun.*, **1999**, 783.

[10] M. A. Palacios, R. McLellan, C. M. Beavers, S. J. Teat, H. Weihe, S. Piligkos, S. J. Dalgarno and E. K. Brechin *Chem. Eur. J.*, **2015**, *21*, 11212.

[11] S. Sanz, R. D. McIntosh, C. M. Beavers, S. J. Teat, M. Evangelisti, E. K. Brechin, S. J. Dalgarno *Chem. Commun.*, **2012**, *48*, 1449.

[12] G. Karotsis, S. Kennedy, S. J. Teat, C. M. Beavers, D. A. Fowler, J. J. Morales, M. Evangelisti, S. J. Dalgarno, E. K. Brechin *J. Am. Chem. Soc.*, **2010**, *132*, 12983.

[13] G. Karotsis, S. Kennedy, S. J. Dalgarno, E. K. Brechin *Chem. Commun.*, **2010**, *46*, 3884.

[14] For an examples see: a) C. Aronica, G. Chastanet, E. Zueva, S. A. Borshch, J. M. Clemente-Juan, D. Luneau *J. Am. Chem. Soc.*, **2008**, *130*, 2365; b) G. Karotsis, S. J. Teat, W. Wernsdorfer, S. Piligkos, S. J. Dalgarno, E. K. Brechin *Angew. Chem.*, **2009**, *121*, 8435; c) G. Karotsis, M. Evangelisti, S. J. Dalgarno, E. K. Brechin *Angew. Chem. Int. Ed.*, **2009**, *48*, 9928; *Angew. Chem.*, **2009**, *121*, 10112; d) S. Sanz, K. Ferreira, R.

D. McIntosh, S. J. Dalgarno, E. K. Brechin, *Chem. Commun.*, **2011**, 47, 9042.

[15] L. T. Carroll, P. Aru Hill, C. Q. Ngo, K. P. Klatt, J. L. Fantini *Tetrahedron*, **2013**, *69*, 5002.

[16] P. Murphy, S. J. Dalgarno, M. J. Paterson *J. Phys. Chem. A*, **2014**, *118*, 7986.

[17] R. McLellan, M. A. Palacios, C. M. Beavers, S. J. Teat, S. Piligkos, E. K. Brechin, S. J. Dalgarno *Chem. Eur. J.*, **2015**, *21*, 2804.

[18] M. Coletta, R. McLellan, A. Waddington, S. Sanz, K. J. Gagnon, S. J. Teat, E. K. Brechin, S. J. Dalgarno *Chem. Commun.*, **2016**, *52*, 14246.

[19] For examples see: a) L. Wang, Y. Li, Y. Peng, Z. Liang, J. Yu, R. Xu *Dalton Trans.*, **2012**, *41*, 6242; b) R. McLellan, J. Rezé, S. M. Taylor, R. D. McIntosh, E. K. Brechin, S. J. Dalgarno *Chem. Commun.*, **2014**, *50*, 2202.

[20] H. Weihe and H.-U. Güdel *J. Am. Chem. Soc.*, **1998**, *120*, 2870.

## Table of Contents

# FULL PAPER

Bis-calix[4]arene is a versatile ligand that have been used to form a new family of 3*d*–4*f* polymetallic clusters. Empirical metal ion binding rules established for calix[4]arene are closely mirrored in this ligand, suggesting that one may use coordination preferences and ligand alteration / design in order to tune both cluster formation and composition at a high level in complex multi-component systems.

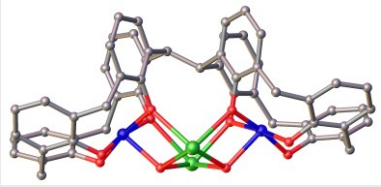

*Marco Coletta, Ross McLellan, Sergio Sanz, Kevin J. Gagnon, Simon J. Teat, Euan K. Brechin* and Scott J. Dalgarno**

**Page No. – Page No.**

**A New Family of 3*d*-4*f* Bis-Calix[4]arene-Supported Clusters**